The Materials Research Society (MRS)

XXII INTERNATIONAL MATERIALS RESEARCH CONGRESS 2013

NACE International Congress-Mexican Section

Eduardo Aguirre de la Torre
Miguel de Cervantes 120, Complejo industrial Chihuahua. C.P. 31109
Tel: 439-11-00
E-mail: eduardo.aguirre@cimav.edu.mx

Cynthia Gómez Esparza
Miguel de Cervantes 120, Complejo industrial Chihuahua. C.P. 31109
Tel: 439-11-00
E-mail: cynthia.gomez@cimav.edu.mx

Javier Camarillo Cisneros
Miguel de Cervantes 120, Complejo industrial Chihuahua. C.P. 31109
Tel: 439-11-00
E-mail: javier.camarillo@cimav.edu.mx

Raúl Pérez Bustamante
Miguel de Cervantes 120, Complejo industrial Chihuahua. C.P. 31109
Tel: 439-11-00
E-mail: raul.perez@cimav.edu.mx

Roberto Martínez Sánchez
Miguel de Cervantes 120, Complejo industrial Chihuahua. C.P. 31109
Tel: 439-11-00
E-mail: roberto.martinez@cimav.edu.mx

EFFECT OF RARE EARTHS ON THE MICROSTRUCTURE AND MECHANICAL PROPERTIES OF THE A356 ALUMINUM ALLOY

Abstract

The research of rare earths for the synthesis of materials with improved mechanical performance is of great interest when they are considered for potential applications in the automotive industry. In this regard, the effect on the mechanical properties and microstructure of the automotive A356 aluminum alloy reinforced with 0.2 (wt.%) Al-6Ce-3La (ACL) was investigated. The ACL was added to the melted A356 alloy in the 1) as-received condition and 2) processed by mechanical milling. In the second route, the effect of the ACL processed by mechanical milling and powder metallurgy techniques was investigated, and compared with the results obtained from the A356 alloy strengthened with ACL in the as-received condition. Microstructural properties were evaluated by means of X-ray diffraction in order to observe the solubility of Ce/La in the Al matrix. In addition, electron microscopy was employed in order to investigate the effect of milling time on the size and morphology of La/Ce phase under milling process. Mechanical properties of the A356 alloy modified with ACL were measured by hardness and tensile test. For comparison unmodified specimens of the A356 were characterized according to the previous procedure. The microstructural and mechanical characterization was carried out in specimens after solution and artificial aging. Observations in scanning electron microscopy indicate a homogeneous dispersion of La/Ce phases by using both routes; however, mechanical results, in the modified A356 alloy with the ACL in the as-received condition, show an improvement in the mechanical performance of the A356 alloy over that reinforced with the ACL mechanically milled.

Keywords: A356; Rare earths; Mechanical milling, Mechanical properties

Introduction

Aluminum-silicon alloys are widely used in automobile industry not only because they are easily castable in complex forms but also because of their excellent wear resistance, light weight plus good strength that make them widely used in the manufacture of numerous automotive parts, such as engine blocks and wheels. Besides that, their mechanical properties can be improved by the additional alloying elements. As part of the aluminum-silicon alloys, the A356 aluminum alloy is extensively used in the automotive industry due to their excellent casting characteristics and resistance to corrosion conditions. It has been studied that its mechanical performance can be improved by the addition of small amount of rare earth (RE) elements, which its importance can produce an extension of its mechanical capabilities [1]. The use of RE such like Er [2], Sc [3], Ce [4-8] and La [9, 10] has been studied with beneficial effects on the mechanical properties of aluminum alloys. However, this reported increments in mechanical properties have been more evident at low concentrations of RE.

The dispersion of a RE-rich phase via liquid route implies the formation of coarse and needle-like phases limiting the amount of RE than can be dispersed in the aluminum [10] and could act as a concentrator of stress. The strengthening effect of dispersoids is based on the obstruction of the matrix dislocation lines movement. The strengthening of dispersoids effectiveness depends on their type, size, morphology, volume fraction and distribution. Their resistance against dissolution in the matrix and coalescence is an important factor in their strengthening effect, mainly at high temperatures [11]. In this concern, needle-like phases typically found in Al-RE alloys must be fragmented to increase their strengthening effect and to avoid coalescence and growth. It is possible to reach a homogeneous dispersion of RE phases by using small concentrations of RE; However, the fragmentation by mechanical methods is another route that can be taken [11, 12].
The objective of this research is the study of the effect on microstructure and mechanical properties of the RE dispersion in melted aluminum. According to this, there are two routes to follow: the A1-RE master alloy fragmented by a milling process and the use of it in the as received condition.

EXPERIMENTAL PROCEDURE

ACL addition to the A356 aluminum alloy

A commercial ACL alloy, composed by 6.0 wt. % of Ce, and 3.0 wt.% of La, was added to the A356 alloy in the as-received and milled condition. Metal shaving from the ACL was mechanically milled in a high energy mill SPEX 8000 for the processing of the ACL by

milling process. The mass of the material for milling was of 8.5 g and a ball-to-material ratio was of 5:1. Milling runs were performed with methanol as a process control agent (PCA). Argon was used as inert atmosphere. The milling time was of 5 and 10 h. Milled powders were cold consolidated into discs of 10 mm of diameter.
Melting of the A356 alloy (chemical composition in Table I) was performed in a crucible furnace at 750°C. The molten alloy was degassed with Ar during 10 min. The ACL alloy in the as-received and milled condition were added with a concentration of 0.2 wt.%. Molten was stirred for a period of 5 min and transferred to a permanent mold where it was cooled at room temperature. Samples were solution heat treated at 540°C during 3 h, quenched in water at 60°C and artificially aged at 165°C for 3 h (T6 condition).

Table I. Chemical composition of the A356 alloy

Element	Si	Fe	Mg	Ti	Sr	Cu	Mn	Zn	Ni	Cr	Al
Wt%	6.398	0.098	0.249	0.097	0.010	0.001	0.003	0.006	0.012	0.001	Bal
±	0.421	0.005	0.015	0.011	0.001	0.000	0.000	0.002	0.001	0.001	

Microstructural and mechanical characterization

The microstructural characterization of the ACL alloy in the as-received (AR) and mechanical milled (M) condition occurred in the following way: the preparation of the cross-section of the ACL for both (AR and M) conditions was carried out with hot mounting samples in Bakelite and then prepared with conventional metallographic techniques. The microstructural characterization of the cross-section of the samples was done by means of scanning electron microscopy (SEM) in a JEOL model JSM 5800-LV operated at 15 kV.

X-ray diffraction (XRD, Panalytical X'Pert PRO with X'Celerator detector, interval from 20 to 140 degrees) analysis was used to study the crystallization behavior. SEM micrographs of the reinforced A356 alloy with the ACL-M and ACL-AR condition were obtained. The interaction of the La/Ce phase and the A356 alloy was studied by transmitting electron microscopy in a JEOL model JEM-2200FS microscope operated at 200 kV. Section for TEM was prepared with a focused ion beam (FIB) by using a model JEM-9320FIB with an Omniprobe 200 nanomanipulator. The zone of analysis was previously identified by means of SEM observations. Mechanical properties were evaluated with tensile tests based on ASTM E8. Experiments were performed in an INSTRON/337 universal testing machine at room temperature using a constant crosshead speed of 0.01 mm/s. Hardness was measured under 200 g load with 14.2 s dwell time on a WILSON/K10 Brinell hardness tester.

Results

Fig. 1 shows the representative Backscattered electron SEM micrographs showing the microstructures from Al-RE master alloy in their different processing conditions, as-received and as-milled for 5 and 10 h. It also shows the cross-sectional of ACL-AR master alloy. The presence of large needles bright phases exceeding 50 µm of length in several zones and composed by La/Ce can be observed it has been shown in the elemental analysis from Fig. 1b. It is observed the presence of tips in needle-like phases, which suggest a stress concentrator, that negatively affect the mechanical properties. Additionally, a gray phase composed by Al is observed. The fragmentation behavior of the ACL-M master alloy due progression in milling time is shown in Figs. 1c and d. A noticeable change in the morphology of the La/Ce phases is observed in Fig. 1c when the ACL-M alloy is under the effect of 5 h of milling. It can be observed a noticeable reduction in the size of the bright phases which is less than 10 µm in diameter. Bright and round La/Ce phases are dispersedly seen and uniformly distributed in the aluminum during this milling time. An extensively reduction in the size of La/Ce phases (bright particles) is achieved reaching a higher degree of homogeneity in the distribution of La/Ce in the aluminum when the milling time is incremented to 10 h. Therefore, an incipient dissolution of La/Ce into aluminum can be expected [12]. This fact suggests that the ACL, which was milled for 10 h, offers the most evident way of comminuting the La/Ce phases because of the milling time employed in this research. In addition, micrographs of the morphology of the as-milled powders for 5 and 10 h are given by an inset into the Figs. 1c and 1d respectively. For both milling conditions particles are equiaxed and with a wide size distribution. Particles under the two milling conditions present a broad distribution in size. However, a narrow distribution in the size of the particles after being milled during 10 h can be appreciated, this corresponds to the reduction in the size of the La/Ce phases observed in their corresponding microstructures and thus the predominance of the welding stage in the fracture-welding-fracture process of the milling process occurs.

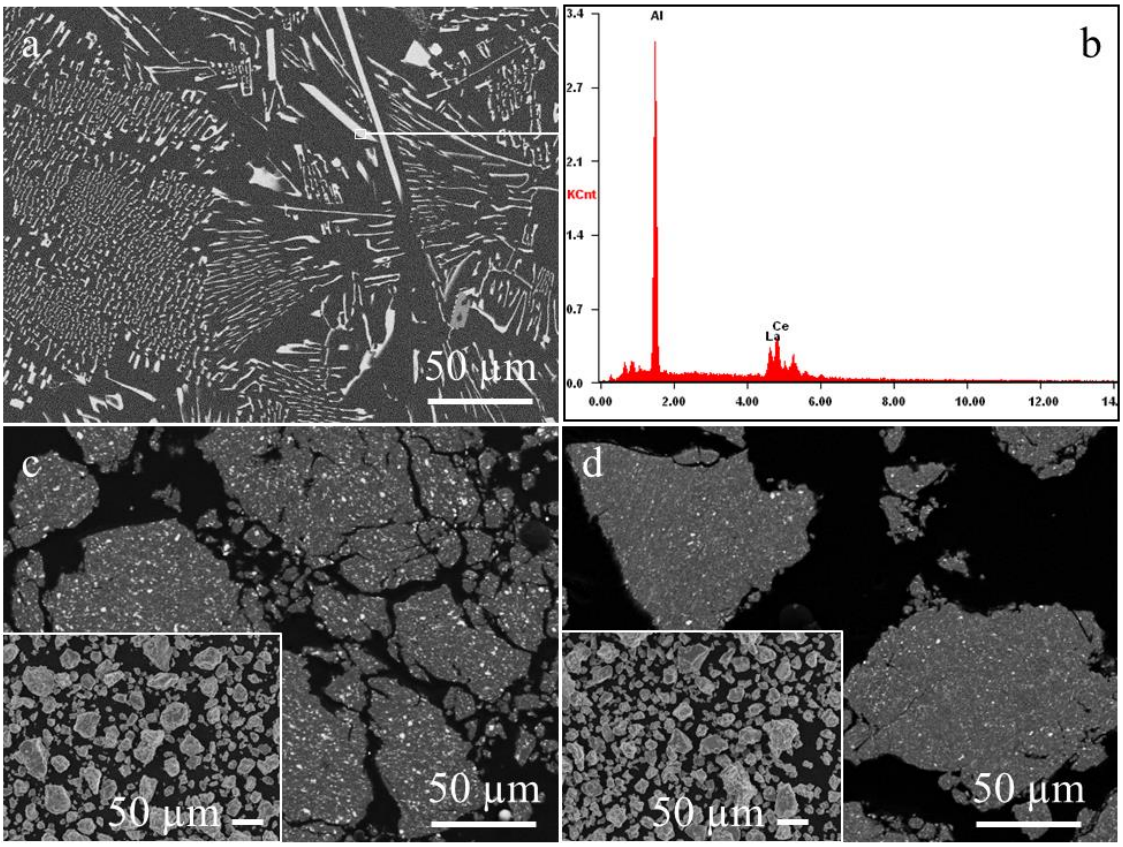

Figure 1. Backscattered electron SEM micrographs of the cross-section of an AC Lmaster alloy. (a) As-received condition, (b) elemental analysis of the bright needle phase presented in the as-received master alloy. ACL master alloy under (c) 5 and (d) 10 h of milling. Secondary electron SEM micrographs show the morphology of the as-milled powders is included in (c) and (d) respectively.

Structural evolution of ACL master alloy during milling process was followed by XRD, patterns are shown in Fig. 2. The ACL-AR alloy was denoted with 0 h in this figure. In this section X-ray diffraction patterns are shown in an ascending array as function of the milling time. Results indicate the presence of four phases, one that corresponds to the aluminum signal and the remaining three phases correspond to compounds containing Ce/La ($AlLa_4$, $CeAlO_3$ and $Al_{11}Ce_3$). Changes in the broadening of the aluminum peaks as consequence of increasing milling time are only visible for the low intensity peaks (larger 2θ values), which indicates a refinement of crystal size. Furthermore the dissolution of the Ce and La compounds in the aluminum matrix is not completely evident, since shift of Al peaks is very small. Additionally they could be not completed dissolved, resulting from the predominance of the welding stage in the fracture-welding process in the milling stage.

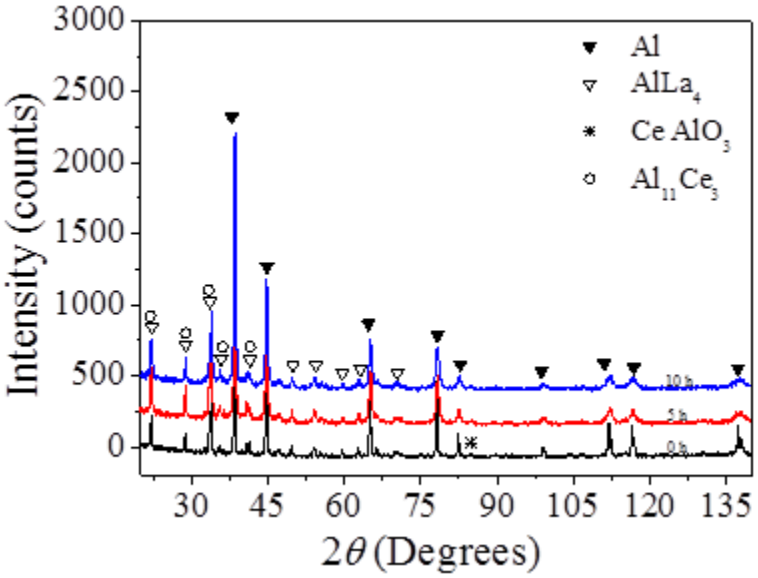

Figure 2. XRD patterns of the ACL master alloy in the as-received (0 h) and as-milled condition (5 and 10 h of milling)

The dispersion of ACL phase is analyzed by SEM in alloys under T6 heat treatment. Fig. 3 shows secondary SEM micrographs of the microstructure after solution and artificial aging of the A356 alloy (Fig. 3a) and the modified A356 alloy with 0.2 wt.% of ACL-M (Fig. 3b) and ACL-R (Fig. 3c). The typical microstructure observed in aluminum-silicon alloys after solution and aging treatment is shown in all micrographs. The presence of RE phases is observed in bright tone and rounded morphology, the aluminum matrix is observed in gray and the spheroidal silicon is observed in dark gray color.

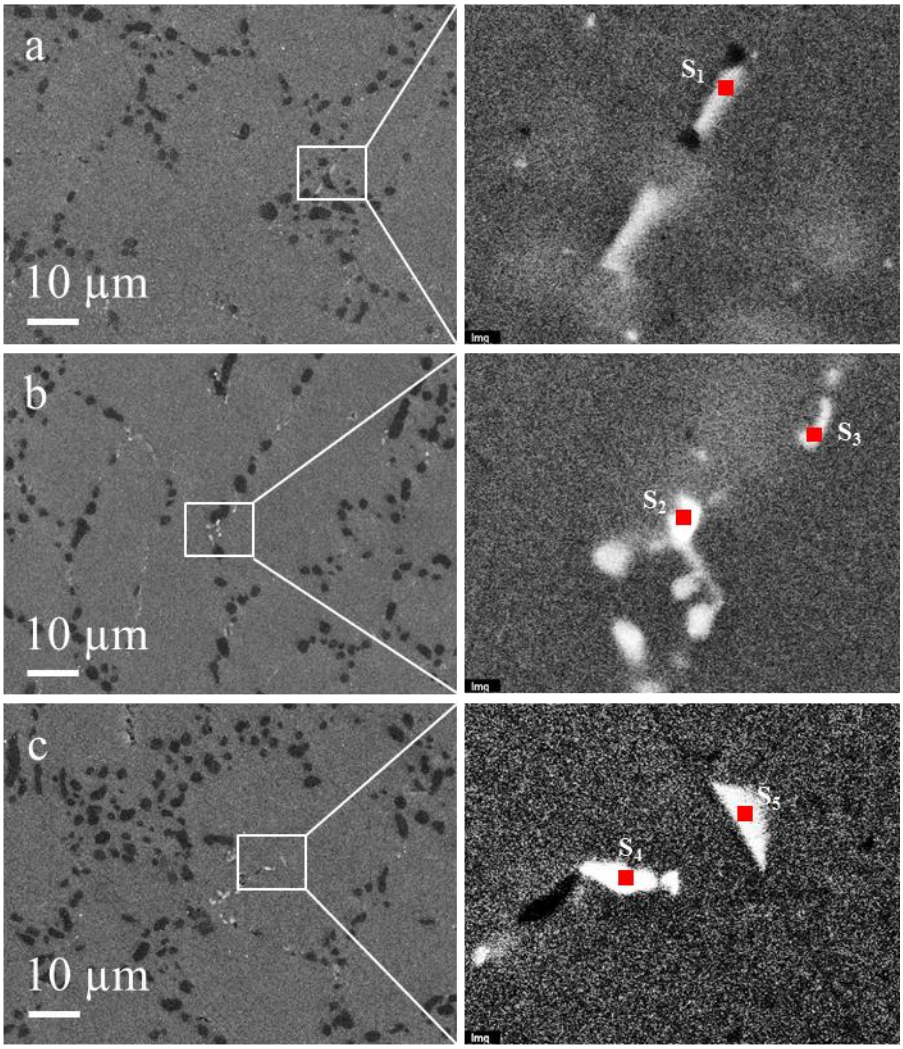

Figure 3. Secondary SEM micrographs. (a) Unreinforced A356 aluminum alloy. (a) A356 aluminum alloy, (b) A356 modified with ACL-M and (c) A356 modified with ACL-AR. All samples were analyzed in the T6 condition. Red squares indicates the EDS analysis zone

The right column shows a magnified view of the selected square, different EDS analyses were carried-out and are reported in Table II. Fig. 3a shows a plaque-like and bright phase, analysis taken in this phase and identified as S1, shows high Fe content (see Table II). Bright and rounded shape phases are observed in the close up from Figs. 3b and 3c. Microanalyses done in the indicated positions by S2, S4 and S5 showed presence of RE in these phases spectrum S3 in Fig. 3b present similar composition to S1.

Table II. Elemental analysis (wt.%) of the selected zones on the A356 and modified A356.

Element	S_1	S_2	S_3	S_4	S_5
AlK	83.60	55.01	74.71	73.44	88.55
SiK	07.59	27.05	18.58	08.15	03.42
FeK	08.81	-	06.71	05.43	01.08
LaL	-	06.53	-	05.94	02.47
CeL	-	11.41	-	08.15	02.70
NiK	-		-	-	01.77

A noticeable fragmentation of the La/Ce phases was achieved after the milling process (Fig. 1). There is no important variation observed in size of the La/Ce phases by comparing 356-ACL-M and 356ACL-AR. Fragmented Ce/LA phases are not prone to growth by coalescence during the dispersion of ACL-M into melted 356 alloy. In the same way, since the ACL-AR concentration is too low, it is expected a partial dissolution and fragmentation during dispersion of ACL-AR into melted aluminum alloy. At the end, Ce/La phases from milled and as received master alloy present a similar size.

It can be noted, that RE phase in the A356 alloy in both ACL-M (Fig. 3b) and ACL-AR (Fig. 3c) condition does not present the La/Ce needle-like shape phases as those observed in Fig. 1a. This suggests that the amount of RE added to 356 is not enough to produce needle-shape phases, which are not recommended because they could act as stress concentration due to their morphology. Furthermore, small additions of RE could lead to a positive effect in the reduction of grain size [4].

Fig. 4 shows a representative sample obtained from the process and the zone of extraction for the TEM specimen. Fig. 4a shows a photograph of the sample and the zone of interest located near the intersection of the lines perpendicularly carved on the sample surface. Figs. 4b and 4c display Ion-induced secondary electron (ISE) images acquired by FIB of the zone previously identified by SEM analysis and taken at the same magnification. Fig. 4c shows a close-up of the interested area. The presence of three phases, corresponding to the aluminum, silicon and La/Ce can be observed. A marked contrast can be noticed between the morphology obtained by SEM, as it was observed in Fig. 2, and ISE images produced by the nature of their acquisition [13]. Fig. 4c shows the zone where the carbon protective layer for the lamella extraction is deposited and the extraction zone is marked with a rectangle in white dotted lines. As it can be observed, the selected zone for extraction contains the presence of the three main phases (Al, Si and La/Ce) involved in the reinforced A356 alloy.

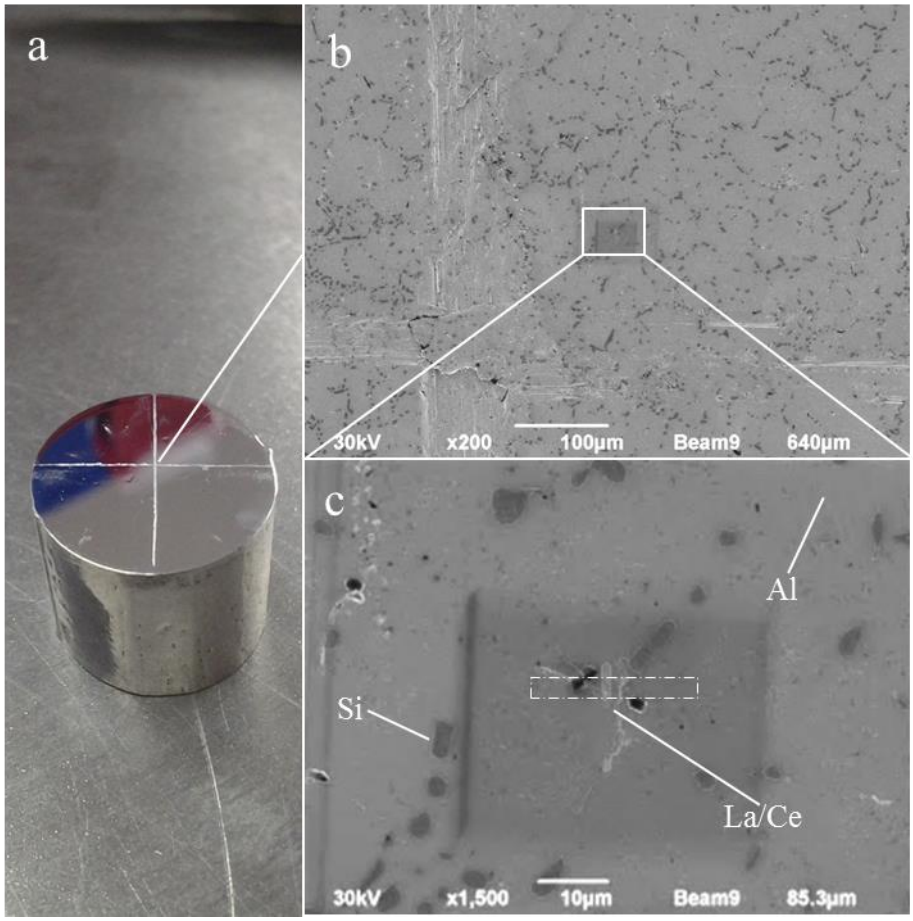

Figure 4. Extraction zone of the TEM sample. (a) Photograph of the zone of analysis. (b-c) ISE images of analysis zone for the lamella extraction.

A bright field STEM micrograph from the FIB-milled TEM sample is presented in Fig. 5. The presence of three phases in different shades of gray can be observed. White squares of five different zones indicate the area of elemental analyses that are shown in Table III. It is corroborated the presence of three phases according to the EDS analyses, where the darkest area correspond to the La/Ce phase. In this concern, a stronger interaction among the phases due to the presence of transition layer among them can be observed. The selected area electro diffraction (SAED) patterns obtained from two different regions (Z_1, Z_2) in the sample are presented and they indicate high crystallinity nature. The selected phases correspond to Aluminum matrix and La/Ce phase. In this matter, the presence of micrometric phases of La/Ce could have a strengthening effect as a second phase and its interaction with grain boundaries. Additionally, since this is a hard phase, it could have an important effect in the arrest of the dislocation lines [4].

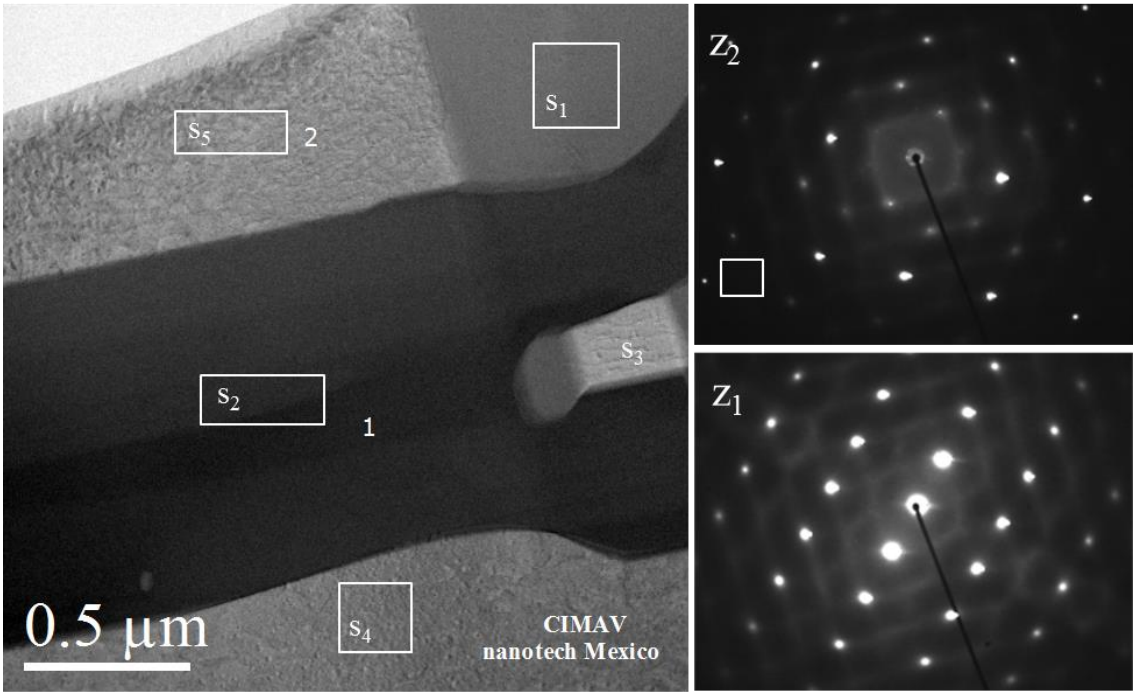

Figure 5. Bright field STEM micrograph of the La-Ce, Si and Al phases. Squares indicates elemental analysis carried out. Circles and isolated numbers indicates the zone where diffraction patterns were taken.

Table III. Elemental analysis of the selected zones in the lamella.

Spectrum	Al	Si	Fe	La	Ce
S_1	56.1	16.2	27.7		
S_2	19.7	21.5		22.3	36.5
S_3	57.0	15.8	27.3		
S_4	97.7	2.3			
S_5	97.4	2.6			

Fig. 6 shows the results from mechanical evaluation in the samples obtained with hardness and a tensile test. Results are presented for all samples in the as-cast and T6 condition in order to observe the effect of La/Ce dopants on the mechanical behavior. Stability in hardness in the as-cast condition for all experiments, which present an average hardness value about 60 Brinell hardness units, can be observed in Fig. 6a; however, the modified A356 alloys display an enhancement in their hardness after T6 heat treatment. Even when the size of La/Ce phases is similar in both dispersion methods (Fig. 3), a slight increase in the hardness values is appreciated in the alloy reinforced with ACL-M (88 HB) over the alloy reinforced with ACL-AR (84 HB). In this concern, an increase in hardness of about 11% by the A356-ACL-M alloy over the unreinforced A356 is obtained. In relation

with the results obtained from the tensile test, a similar behavior is observed in the alloys in the as-cast condition, where the lowest value in σ_y is observed in the A365-ACL-M with 90 MPa. In this matter, the highest value is reached by the unreinforced A356 (94 MPa). However, after T6 treatment condition, a noticeable increase in σ_y is presented by the alloys modified with ACL over the reference A356 alloy. The maximum value is presented in the A356 alloy reinforced with ACL-AR. Nevertheless, the alloy reinforced with ACL-M display a σ_y value of 184 MPa, which represent an increase in σ_y of 15 % over the unmodified A356 alloy. Even though hardness, σ_y and σ_{max} have been improved by the addition of Ce/La; the elongation (ε) does not present significant changes in the as-cast and T6 condition. The above observations suggest the possibility of a greater interaction of the La/Ce phases with the precipitates produced during heat treatment as it was investigated by Xiao *et al* [14], where the reinforcement of an Al–Cu–Mg–Ag alloy reinforced with 0.2 wt.% of Ce induced the precipitation of coarser and denser precipitates and as consequence improving the tensile strength of the heat treatable alloys. In this concern, a noticeable increase in the mechanical performance of the A356 modified with ACL in both processing conditions used in this study (ACL-AR and ACL-M) can be observed. In addition, it must be noticed that an increase in the mechanical behavior of the A356 was reached by the use of 0.2 wt.% of ACL, which content of La/Ce is of 9.0 wt.%. However, further analyses about the mechanical behavior of the A356 alloy reinforced with ACL-M must be carried out.

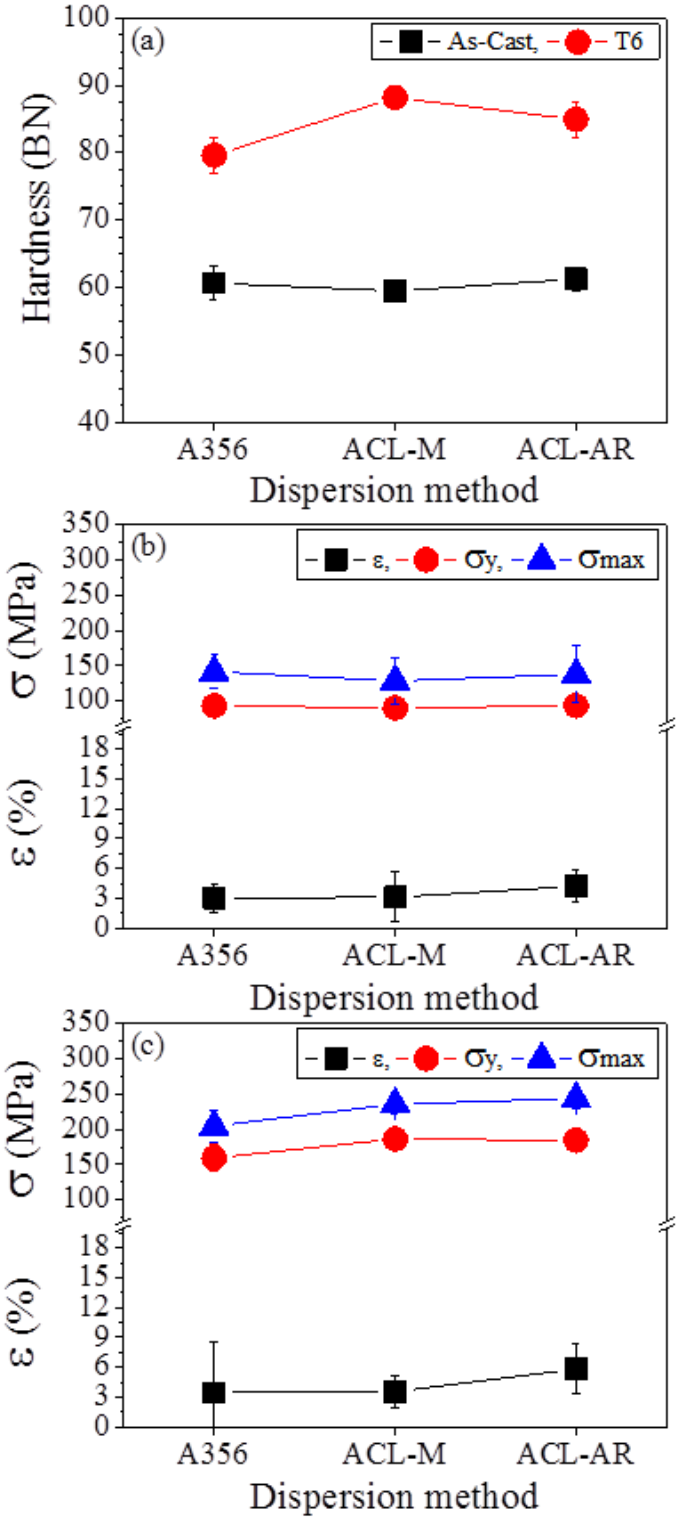

Figure 6. Results from mechanical properties. (a) Hardness results, (b) tensile in the as-cast and (c) T6 condition.

Conclusions

- An ACL master alloy was mechanically milled and then dispersed into a molten A356 alloy.
- The finer fragmentation in the La/Ce phase into the ACL master alloy was obtained at 10 h of milling.
- The A356 alloy reinforced with 0.2 wt. % of ACL master alloy was microstructurally characterized by electron microscopy. The La/Ce phases in the A356 alloy are similar in size for both ACL-AR and ACL-M dispersion method
- An increase in hardness of about 11 % was observed in the A356-ACL-M over the unreinforced alloy. In this concern, an increase in σ_y of about 15 % was presented in the A356-ACL-AR over the unmodified A356 alloy.
- According to the results a further increase in the ACL concentration beyond 0.2 wt.% can be carried out with the possibility of increasing the mechanical behavior of the A356 alloy.
- From the above considerations, it is suggested that an increase in the mechanical performance of the alloy can be achieved produced by a homogeneous dispersion of fine particles containing La/Ce phase.
- Further investigation of the milling time for the processing of the amount of ACL master alloy that can be added in the A356 alloy produced by milling routes must be considered.

Acknowledgements

The authors of this research would like to thank to K. Campos-Venegas. O. Solis-Canto, E. Torres-Moyé and C.E. Ornelas-Gutierrez for their valuable technical assistance. J. Camarillo-Cisneros are grateful for partial support from CONACYT via PhD scholarship 290674 and 290604.

References

[1] Wang S, Zhou H, Kang Y, The influence of rare earth elements on microstructures and properties of 6061 aluminum alloy vacuum-brazed joints, *J. Alloys Comp.*, 2003, **352**(1-2): 79-83.

[2] Hu X, Jiang F, Ai F, Yan H, Effects of rare earth Er additions on microstructure development and mechanical properties of die-cast ADC12 aluminum alloy, *J. Alloys Comp.*, 2012, **538**(0): 21-27.

[3] Prukkanon W, Srisukhumbowornchai N, Limmaneevichitr C, Influence of Sc modification on the fluidity of an A356 aluminum alloy, *J. Alloys Comp.*, 2009, **487**(1-2): 453-457.

[4] Zhang J, Yu P, Liu K, Fang D, Tang D, Meng J, Effect of substituting cerium-rich mischmetal with lanthanum on microstructure and mechanical properties of die-cast Mg-Al-RE alloys, *Mater. Des.*, 2009, **30**(7): 2372-2378.

[5] Pengfei L, Zhigang W, Yunli W, Xizhu G, Zaiyun W, Zhiqiang L, Effect of Cerium on Mechanical Performance and Electrical Conductivity of Aluminum Rod for Electrical Purpose, *J. Rare Earths*, 2006, **24**(1, Supplement 1): 355-357.

[6] Govindaraju H K, Jayaraj T, Sadanandarao P R, Venkatesha C S, Evaluation of mechanical properties of as-cast Al-Zn-Ce alloy, *Mater. Des.*, 2010, **31, Supplement 1**(0): S24-S29.

[7] Chen Z, Chen P, Li S, Effect of Ce addition on microstructure of Al20Cu2Mn3 twin phase in an Al-Cu-Mn casting alloy, *Mater. Sci. Eng., A*, 2012, **532**(0): 606-609.

[8] Kiyota S, Valdez B, Stoytcheva M, Zlatev R, Bastidas J M, Anticorrosion behavior of conversion coatings obtained from unbuffered cerium salts solutions on AA6061-T6, *J. Rare Earths*, 2011, **29**(10): 961-968.

[9] Zhang G-j, Liu G, Sun Y-j, Jiang F, Wang L, Wang R, Sun J, Microstructure and strengthening mechanisms of molybdenum alloy wires doped with lanthanum oxide particles, *Int. J. Refract. Met. Hard Mater.*, 2009, **27**(1): 173-176.

[10] Tsai Y-C, Chou C-Y, Lee S-L, Lin C-K, Lin J-C, Lim S W, Effect of trace La addition on the microstructures and mechanical properties of A356 (Al-7Si-0.35Mg) aluminum alloys, *J. Alloys Comp.*, 2009, **487**(1-2): 157-162.

[11] Santos-Beltran A, Gallegos-Orozco V, Estrada-Guel I, Bejar-Gómez L, Espinosa-Magaña F, Miki-Yoshida M, Martínez-Sánchez R, TEM characterization of Al-C-Cu-Al2O3 composites produced by mechanical milling, *J. Alloys Comp.*, 2007, **434-435**(0): 514-517.

[12] Suryanarayana C, Ivanov E, Boldyrev V V, The science and technology of mechanical alloying, *Mater. Sci. Eng., A*, 2001, **304-306**(0): 151-158.

[13] Volkert C A, Minor A M, Focused Ion Beam Microscopy and Micromachining, *MRS Bull.*, 2007, **32**(1): 389-399.

[14] Xiao D H, Wang J N, Ding D Y, Yang H L, E ffect of rare earth Ce addition on the microstructure and mechanical properties of an Al–Cu–Mg–Ag alloy, *J. Alloys Comp.*, 2003, **352**(1): 84-88.